A pRb-responsive, RGD-modified, and Hyaluronidase-armed Canine Oncolytic Adenovirus for Application in Veterinary Oncology

Eduardo Laborda[1,2], Cristina Puig-Saus[1], Alba Rodriguez-García[1], Rafael Moreno[1], Manel Cascalló[3], Josep Pastor[4] and Ramon Alemany[1]

[1]Translational Research Laboratory, IDIBELL-Institut Català d'Oncologia, Barcelona, Spain; [2]Biochemistry and Molecular Biology Department, Autonomous University of Barcelona, Barcelona, Spain; [3]VCN Biosciences, Barcelona, Spain; [4]Animal Medicine and Surgery Department, Fundació Hospital Clínic Veterinari, Autonomous University of Barcelona, Barcelona, Spain

Human and canine cancer share similarities such as genetic and molecular aspects, biological complexity, tumor epidemiology, and targeted therapeutic treatment. Lack of good animal models for human adenovirotherapy has spurred the use of canine adenovirus 2-based oncolytic viruses. We have constructed a canine oncolytic virus that mimics the characteristics of our previously published human adenovirus ICOVIR17: expression of E1a controlled by E2F sites, deletion of the pRb-binding site of E1a, insertion of an RGD integrin-binding motif at the fiber Knob, and expression of hyaluronidase under the major late promoter/IIIa protein splicing acceptor control. Preclinical studies showed selectivity, increased cytotoxicity, and strong hyaluronidase activity. Intratumoral treatment of canine osteosarcoma and melanoma xenografts in mice resulted in inhibition of tumor growth and prolonged survival. Moreover, we treated six dogs with different tumor types, including one adenoma, two osteosarcomas, one mastocitoma, one fibrosarcoma, and one neuroendocrine hepatic carcinoma. No virus-associated adverse effects were observed, but toxicity associated to tumor lysis, including disseminated intravascular coagulation and systemic failure, was found in one case. Two partial responses and two stable diseases warrant additional clinical testing.

Received 18 April 2013; accepted 14 January 2014; advance online publication 4 March 2014. doi:10.1038/mt.2014.7

INTRODUCTION

In dogs as in humans, cancer is a major cause of mortality.[1,2] More than four million new cancer diagnoses in pet dogs are expected per year.[2] Virotherapy with conditionally replicative viruses in general, adenovirus (Ad) in particular is a promising therapy for cancer.[3] Several animal species have been used as models for cancer therapy with human Ad (hAd).[4] Often, xenograft-implanted nude mice are used to analyze efficacy and immune-competent mice are used for toxicity.[5] However, the mouse is nonpermissive to hAd replication. Syrian Hamster has been suggested as a better model than mouse[6] because it is semipermissive to hAd replication. Despite this advantage, hamster tumors are still engrafted showing a structure and progression different from that of spontaneous tumors. These fundamental differences lead to poor preclinical to clinical correlations in efficacy and, occasionally, to nonexpected toxicity events.[7]

HAd5 replication has been demonstrated in established and primary canine cell lines[8] pointing the dog as a good model to analyze preclinically human conditionally replicative Ads (CRAds). Moreover, an immune-stimulatory human vector (AdCD40L) has been administered in canine melanoma patients with promising results, warranting future application in human patients.[9] In this context, the dog has been suggested as an ideal syngeneic model for virotherapy. Pet dogs develop cancer spontaneously due to an increased life expectancy and an exposure to similar environmental conditions to humans.[10] Canine patients provide an outbred genetic background and they are genetically closer to humans than laboratory rodents.[11] Moreover, cancer therapy occurs in the presence of an immune system and the biologic behavior and clinical presentation of certain canine tumors are similar to their human counterparts.[2] Dogs are routinely vaccinated with canine adenovirus type 2 (CAV2)-based vaccines[12] to elicit a crossreacting protection against CAV1.[13] Thus, dogs have variable titers of specific neutralizing antibodies resembling human population, with implications for the efficacy and safety of the treatment.[14] With the aforementioned, treatment of pet-dog patients with a canine CRAd (cCRAd) based on CAV2 would fulfill the requirements of a good predictive model of human cancer treatment.[15] On the other hand, cCRAds may benefit canine cancer patients as nearly all cancer treatments for dogs are palliative[1] and around 50% of dogs older than 10 years diagnosed with cancer die because of it.[2] Developing new cancer therapies for canine patients may bring veterinary medicine at the forefront of cancer therapy research.

With this aim, an osteocalcin (OC) promoter-controlled cCRAd (OCCAV) has been developed and used to treat canine xenografts.[16,17] OCCAV has proven safe in laboratory Beagles intravenously injected with up to 2×10^{12} viral particles (vp)[18]: only one Grade 4 neutropenia was described, with no other important abnormalities. Necropsies did not show evidence of splenic or

Correspondence: Ramon Alemany, Translational Research Laboratory, IDIBELL-Institut Català d'Oncologia, Av Gran Via de l'Hospitalet 199–203, L'Hospitalet de Llobregat, 08907 Barcelona, Spain. E-mail: ralemany@iconcologia.net

hepatic destruction even when biodistribution pointed out these organs as the main targeted tissues. However, OCCAV efficacy in tumor-suffering dogs remains to be studied and the selective replication in OC-expressing cells will limit the number of patients eligible for treatment.

Our group has previously generated ICOVIR17, an oncolytic Ad based on hAd5, with good results in preclinical studies.[19] In the present study, we developed ICOCAV17, a CAV2-based cCRAd with similar characteristics to ICOVIR17, and two parental viruses, CAV2RGD and ICOCAV15, homologous to their human counterparts AdwtRGD and ICOVIR15, respectively.[20,21] *In vitro* assays showed functional bioactivity of cCRAds and preclinical studies in tumor-harboring nude mice proved intratumoral injection as a safe and effective administration route. However, intravenous toxicity in mice showed marked thrombocytopenia and loss of body weight. Thus, the intratumoral route was chosen for the treatment of six canine patients with ICOCAV17. Results include two partial responses (PR), two stable diseases, and two progressive diseases.

RESULTS

In vitro characterization of cell lines and cCRAds

A schematic representation of the viruses used in this study is shown in **Figure 1a**. All viruses rendered similar yields (9,000 to 10,090

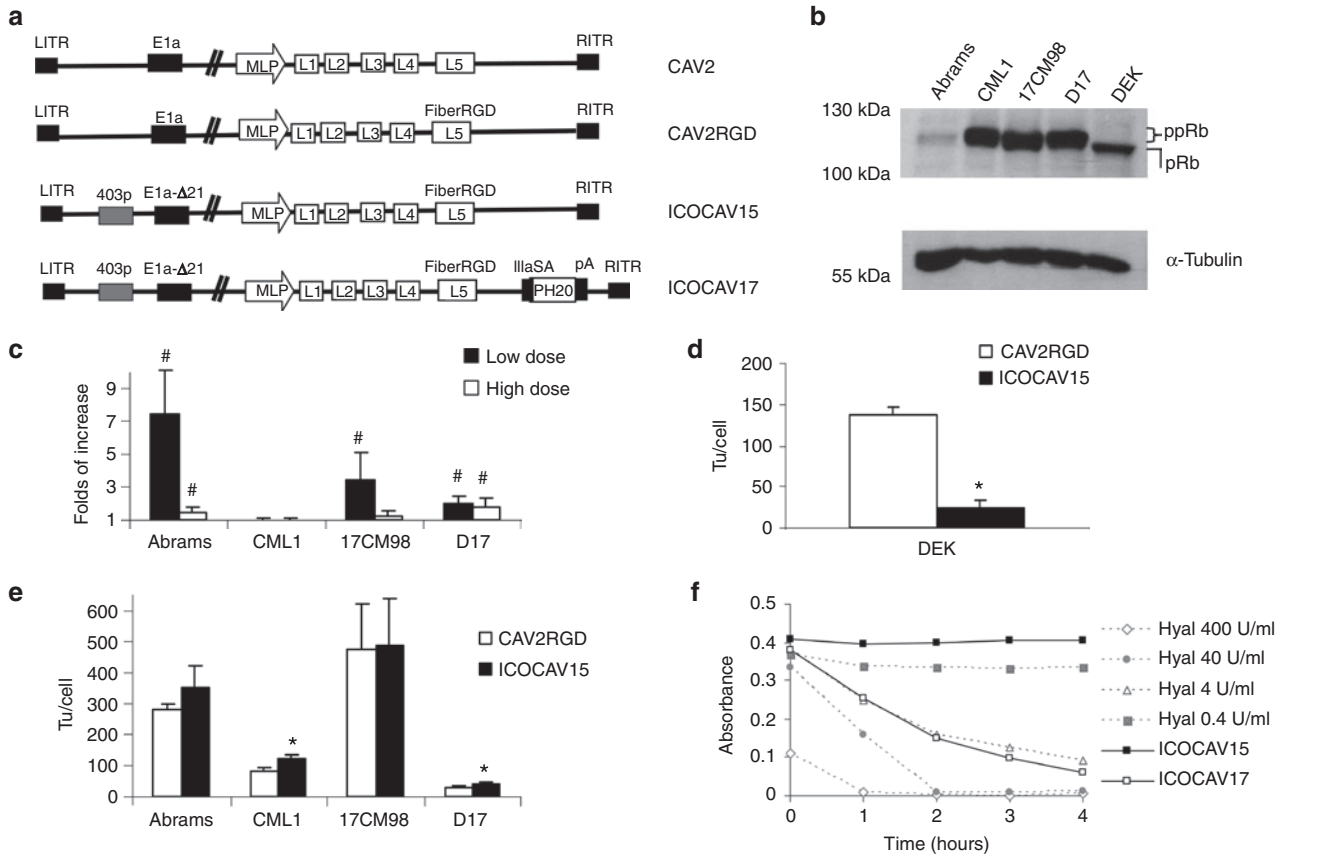

Figure 1 Adenoviruses and cells used in this study and *in vitro* characterization. (**a**) Schematic representation of viruses used in this study. CAV2 is the canine wild-type virus serotype 2. CAV2RGD contains an RGD motif (FiberRGD) in the HI-loop of the CAV2 fiber. ICOCAV15 and ICOCAV17 are canine conditionally replicative adenoviruses, based on CAV2RGD, in which the endogenous E1a promoter have been modified inserting four palindromic E2F-binding sites and one Sp-I-binding site (403p) at the 403 nucleotide position of the virus genome, 21 base pairs of E1a region (E1aΔ21) homologous to Δ24 in human oncolytic adenoviruses have been deleted. ICOCAV17 is armed with the human PH20 hyaluronidase (PH20) under the control of the canine IIIa protein Splicing Acceptor (IIIaSA). MLP, Major late promoter; pA, polyadenylation signal. (**b**) Western blot of pRb in canine tumor cells and dog epidermal keratinocytes (DEK). Both hypophosphorylated (pRb) and hyperphosphorylated (ppRb) forms of the protein were resolved. Abrams cell line expressed low levels of ppRb. α-Tubulin was used as loading control. (**c**) Comparison of infectivity between CAV2 and CAV2RGD in four canine tumor cell lines. Abrams, 17CM98, D17, and CML1 cells were infected with an equal number of viral particles per cell of each virus using two different doses. Immune staining against viral hexon protein was performed 24 hours after infection, and the number of infected cells counted. The ratio between CAV2RGD and CAV2 of three independent assay results ± SD is shown. (**d**) ICOCAV15 total production yields in a cycle-arrested nontumor canine cell line. DEK were seeded in 24-wells plates. After 20 days in confluence, DEK were infected with 8 transducing units (tu)/cell of CAV2RGD or ICOCAV15. Two days postinfection, total virus production was measured. Three independent assay results ± SD are shown. (**e**) Virus production of ICOCAV15 in tumor cells. Different tumor cell lines were infected with a dose of virus that resulted in >80% transduction (20 tu/cell for D17 and CML1 and 30 tu/cell for Abrams and 17CM98). Two days after infection, total virus production was measured in triplicate. Results ± SD are shown. (**f**) Hyaluronidase expression in cells infected with ICOCAV17. DK28Cre cells were infected with ICOCAV15 or ICOCAV17 with 20 tu/cell. After 48 hours, supernatants from infected cells were incubated with a solution of Hyaluronan (HA) for 0, 1, 2, 3, or 4 hours and analyzed. Four samples with known concentration of purified hyaluronidase were used as references. HA degradation was measured by absorbance (600 nm). #Statistical significance between CAV2 and CAV2RGD ($P < 0.05$) by two-tailed unpaired Student's *t*-test; *Statistical significance between CAV2RGD and ICOCAV15 ($P < 0.05$) by two-tailed unpaired Student's *t*-test.

vp/cell) in DK28Cre cells.[22] To test the function of these cCRAds, *in vitro* assays were performed in four canine tumor cell lines. Abrams and D17 (pulmonary metastasis) derive from osteosarcoma (OS),[23] and 17CM98 and CML1 from melanoma.[24] Dog epidermal keratinocytes (DEK) were used as nontumor control cells. Studies point pRb pathway as necessary to cause cancer.[25,26] We characterized pRb status of the cell lines used in this study by western blot (**Figure 1b**). Tumor cells contained hyperphosphorylated pRb (ppRb). In contrast, pRb from DEK was hypophosphorylated (pRb). Additionally, tumor cells were analyzed for expression of Coxsackie virus and adenovirus receptor (CAR) (data not shown). All cells had detectable levels of CAR. CML1 and D17 expressed similar levels to DK28Cre, while 17CM98 expressed lower levels and Abrams expressed even higher levels than DK28Cre. The insertion of RGD at the fiber HI-loop of hAds enhances infectivity and allows the virus to infect cells CAR independently.[20,27] Similarly, CAV2RGD showed enhanced infectivity compared to CAV2 (**Figure 1c**). When we infected cells with a dose of 20 vp/cell for Abrams, 10 vp/cell for 17CM98, 2 vp/cell for D17, and 6 vp/cell for CML1, the infectivity was increased 7.4 times ($P = 0.008$), 3.4 times ($P = 0.04$), and 2 times ($P = 0.03$) in Abrams, 17CM98, and D17 cells, respectively. When infecting with a fivefold higher dose for Abrams, 17CM98, and D17 and a twofold higher dose for CML1, the infectivity was increased 1.4 times ($P = 0.03$), 1.15 times ($P = 0.2$), and 1.7 times ($P = 0.009$) in Abrams, 17CM98, and D17 cells, respectively. No differences were seen in CML1 cells at any dose. To test E2F-driven selectivity, progeny virus production was analyzed in tumor cells and arrested[28] DEK. In DEK, the progeny production of ICOCAV15 showed a decrease of 84% ($P = 0.03$) compared with the parental virus CAV2RGD (**Figure 1d**). Conversely, virus progeny production was increased for ICOCAV15 compared with CAV2RGD in two out of four tumor cell lines (CML1 ($P = 0.008$) and D17 ($P = 0.02$)), and a trend for improved production was observed in the other two cell lines (Abrams and 17CM98; **Figure 1e**). To confirm the activity of the hyaluronidase of ICOCAV17, a hyaluronic acid (HA) degradation assay[29] was performed (**Figure 1f**). Supernatants (SN) from cells infected with ICOCAV17 degraded HA to an equivalent level of 4 units/ml of hyaluronidase, while ICOCAV15 SN did not degrade HA at all. Finally, cytotoxicity was analyzed at days 6–8 comparing all viruses simultaneously (**Figure 2**). Under the conditions of time and transducing units (tu)/cell used, CAV2 was not able to induce cytotoxicity (evidence of cytopathic effect) in Abrams and 17CM98 cells, even at a dose of 2,000 tu/cell. In D17 cells, CAV2RGD decreased the IC_{50} (amount of virus needed to reduce the cell culture viability by 50%) 1.9-fold ($P = 0.032$) compared to CAV2. The E2F-binding sites rendered ICOCAV15 more

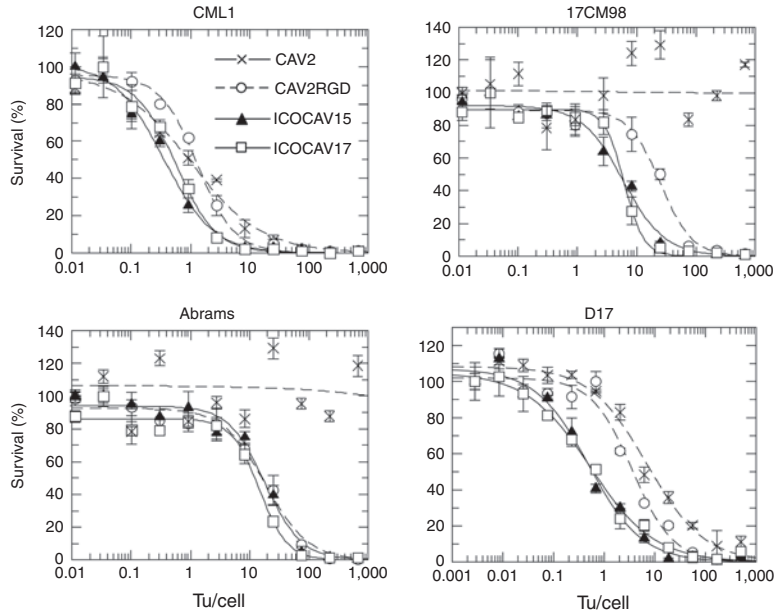

IC50	CAV2	CAV2RGD	ICOCAV15	ICOCAV17
CML1	1.03 ± 0.31	1.30 ± 0.11	0.35 ± 0.04* #	0.57 ± 0.07* #
17CM98	∞	25.01 ± 3.70*	5.9 ± 0.79* #	6.1 ± 0.62* #
Abrams	∞	18.48 ± 2.74*	18.09 ± 2.69*	14.61 ± 2.07*
D17	7.02 ± 1.24	3.59 ± 0.79*	0.49 ± 0.09* #	0.53 ± 0.08* #

Figure 2 Comparative cytotoxicity of canine viruses in four canine tumor cell lines. Infection with the indicated viruses, at doses ranging from 2,000 to 0.01 transducing units (tu)/cell for Abrams, CML1, and 17CM98 or from 500 to 0.001 tu/cell for D17 was performed. The IC50 values (tu/cell needed to reduce by 50% the cell viability) at days 6–8 after infection are shown. Three different replicates were quantified for each cell line. Mean ± SD are plotted. IC50 →∞ for CAV2 at 17CM98 and Abrams cells indicates estimated values of IC50 over 10^6 tu/cell. *Significant ($P < 0.05$) compared to CAV2 by two-tailed unpaired Student's *t*-test; #Significant ($P < 0.05$) compared to CAV2RGD by two-tailed unpaired Student's *t*-test.

cytotoxic decreasing the IC_{50} by 3.7 times ($P = 0.013$), 7.2 times ($P = 0.0009$), and 4 times ($P = 0.005$) in CML1, D17, and 17CM98, respectively, compared to CAV2RGD. ICOCAV17 showed similar IC_{50} values to ICOCAV15. No differences between CAV2RGD, ICOCAV15, and ICOCAV17 were seen in Abrams cells.

Toxicity and biodistribution profile of canine adenoviruses after systemic administration in Balb/C immunocompetent mice

We had previously determined a tolerable dose for wild-type viruses (CAV2 and CAV2RGD) and a peak of body weight loss at day 2 after systemic administration (data not shown). Thus, mice were intravenously injected with 1×10^{11} vp of ICOCAV17 or control viruses. Body weight was monitored daily and overall survival, liver enzymes (aspartate aminotransferase and alanine aminotransferase), and hematology were determined at day 3 after viral injection. At that time, animals were sacrificed and organs of groups injected with CAV2 and CAV2RGD were collected and analyzed for presence of virus.

As expected, weight loss showed a peak of toxicity 48 hours postinjection for all viruses (**Figure 3a**). No animal died or lost more than 10% of its body weight. Viruses with the RGD motif in the capsid induced a significant decrease of body weight compared to CAV2. Moreover, animals injected with ICOCAV15 or ICOCAV17 had a slower recovery than those injected with CAV2RGD. Hematology analysis showed a dramatic decrease in platelets for all viruses (**Figure 3b**). Compared to phosphate-buffered saline, all viruses induced a significant lymphopenia and a modest but significant increase of basophils, whereas only CAV2RGD and ICOCAV17 decreased monocytes significantly (**Figure 3c**).

Although a mild increase of liver enzymes was observed, none of the viruses increased significantly alanine aminotransferase or aspartate aminotransferase compared to PBS group (**Figure 3d**), consistent with the biodistribution results, where we did not find a marked liver tropism (**Figure 3e**). Instead, CAV2 and CAV2RGD showed a heterogeneous tropism. The spleen, lungs, liver, and kidney showed the highest concentrations of CAV2 and

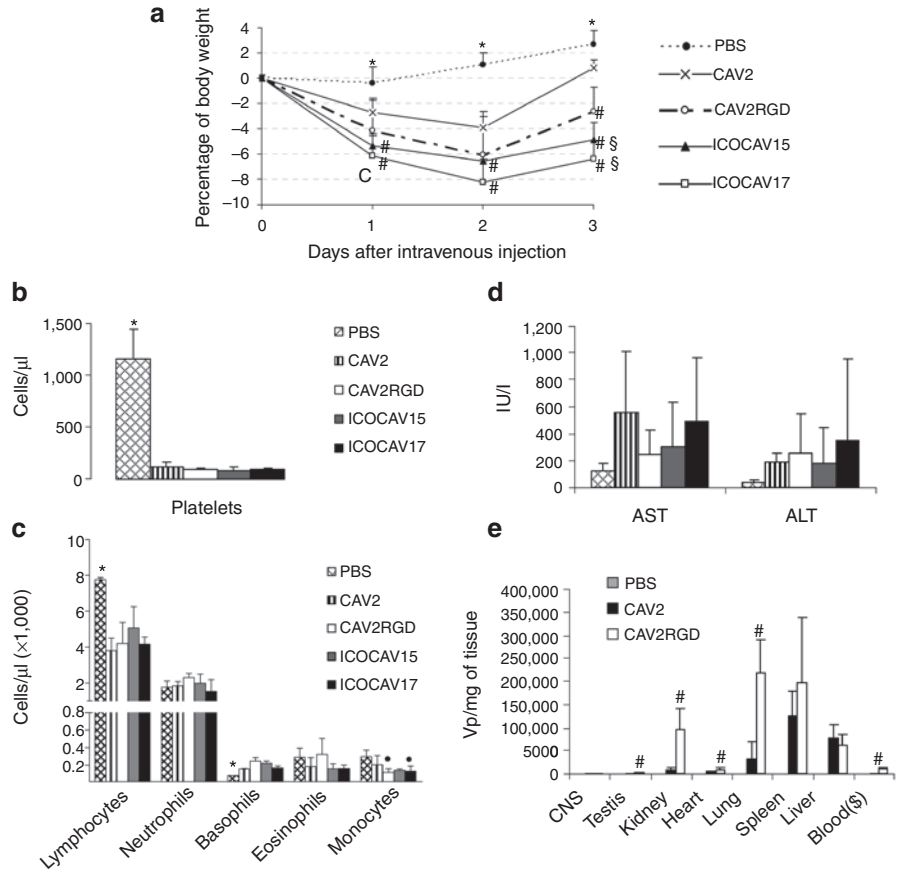

Figure 3 Toxicity and biodistribution profile after systemic administration of canine adenoviruses in immunocompetent mice. Balb/C immunocompetent mice were injected intravenously with PBS or 1×10^{11} viral particles of CAV2, CAV2RGD, ICOCAV15, or ICOCAV17. The average values for (**a**) percentage of body weight variation during all the experiment and (**b**) platelet concentration, (**c**) leukocyte concentration, and (**d**) serum transaminases at day 3 after administration. (**e**) Biodistribution of CAV2 and CAV2RGD in mice tissues. Tissues were harvested 3 days after administration, snap frozen, and quantitatibe polymerase chain reaction assayed for the presence of viruses. Results are reported as viral genomes per milligram of tissue. ($) Blood concentration is reported as viral genomes per milliliter of blood. Mean values ± SD of $n = 5$ mice/group are depicted. *Statistical significance compared with groups injected with viruses ($P < 0.05$) by two-tailed unpaired Student's *t*-test. #Statistical significance compared with CAV2 ($P < 0.05$) by two-tailed unpaired Student's *t*-test. §Statistical significance compared with CAV2RGD ($P < 0.05$) by two-tailed unpaired Student's *t*-test.·Statistical significance compared with PBS ($P < 0.05$) by two-tailed unpaired Student's *t*-test. ALT, alanine aminotransferase; AST, aspartate aminotransferase; CNS, central nervous system; PBS, phosphate-buffered saline.

CAV2RGD (vp/mg of tissue and vp/ng of total DNA), whereas the liver showed the highest absolute amount of viral genomes (**Supplementary Table S1**). The levels of CAV2RGD were higher than those of CAV2 in the testis, heart, lungs, and kidneys. The viremia at day 3 was 100-fold higher for CAV2RGD compared with CAV2.

ICOCAV17 oncolytic potency in two xenograft models

We evaluated ICOCAV17 efficacy in melanoma and OS tumor models (**Figure 4**), two of the most common and devastating cancers in dogs.[30] Nude mice harboring CML1 or Abrams tumors were injected intratumorally three times (on days 0, 7, and 14) with PBS or a dose of 1×10^{10} vp/tumor of each virus. Intratumoral injections did not decrease animal weight. In Abrams, ICOCAV17 decreased tumor volume at the end of the experiment compared to all other groups (1.52-fold ($P = 0.038$) compared to PBS, 1.91-fold ($P = 0.039$) compared to CAV2, 1.87-fold ($P = 0.006$) compared to CAV2RGD, and 1.67-fold ($P = 0.01$) compared to ICOCAV15). In CML1, ICOCAV17 reduced tumor volume fivefold ($P = 0.04$) and 2.7-fold ($P = 0.002$) compared to PBS and CAV2, respectively, at the end of the experiment (day 21 for PBS and day 26 for CAV2). Although differences in tumor volume between ICOCAV15 and PBS groups did not reach statistical significance in CML1, they did when percentage of tumor growth was analyzed at days 7 ($P = 0.02$) and 12 ($P = 0.03$) (data not shown). ICOCAV17 injection increased the survival of Abrams tumor-bearing mice compared to PBS ($P = 0.044$), CAV2 ($P = 0.009$), CAV2RGD ($P = 0.004$), and ICOCAV15 ($P = 0.005$), and compared to PBS ($P = 0.01$) and CAV2 ($P = 0.004$) in CML1 tumor-bearing mice. ICOCAV15 prolonged ($P = 0.058$) the mean survival from 13 and 15 days to 20.5 days, compared to PBS and CAV2 groups, respectively, in the CML1 model. Staining of tumors against late Ad proteins was performed at the end of the experiment (**Supplementary Figure S1 and Supplementary Materials and Methods**). We were able to detect virus in 1 or 2 tumors from each group and a trend for increased dissemination of ICOCAV17 compared with the other groups was observed, primarily in Abrams tumors. After efficacy and toxicity studies in mice, six canine patients were enrolled in an investigational trial with ICOCAV17 (see **Table 1** for a summary of all six cases):

Clinical case I. A 14-year-old entire male Husky that had received surgery 2 years before to remove a sweat gland adenoma, was admitted to the Veterinary Hospital with a mass located at the prepuce skin that caused dysuria. Infiltrative sweat gland adenoma was diagnosed by fine needle aspiration. Due to the poor general condition of the dog and poor benefit of second-line chemotherapy for recurrent sweat gland adenoma,[31] chemotherapy and surgical treatment were declined. The dog was selected for investigational therapy with ICOCAV17.

Treatment and response: physical examination showed a general poor body condition and hind leg weakness. Biochemistry and hematological analysis were within normal limits. ICOCAV17 was injected in four points of the adenoma mass. One day after injection, mild temporal bleeding in one out of four administration points was observed. Fever was detected on day 21 after treatment associated to an anal sac abscess which was controlled with broad spectrum antibiotics. Biochemistry, coagulation, and hematological analysis and physical examination showed no signs of systemic toxicity through all the treatment. Tumor progressively decreased in size and dysuria disappeared within 3 days after virus administration. For at least 6 months, the tumor was in PR with a decrease of 51% in size (**Figure 5**). In the last check-up, 11 months after

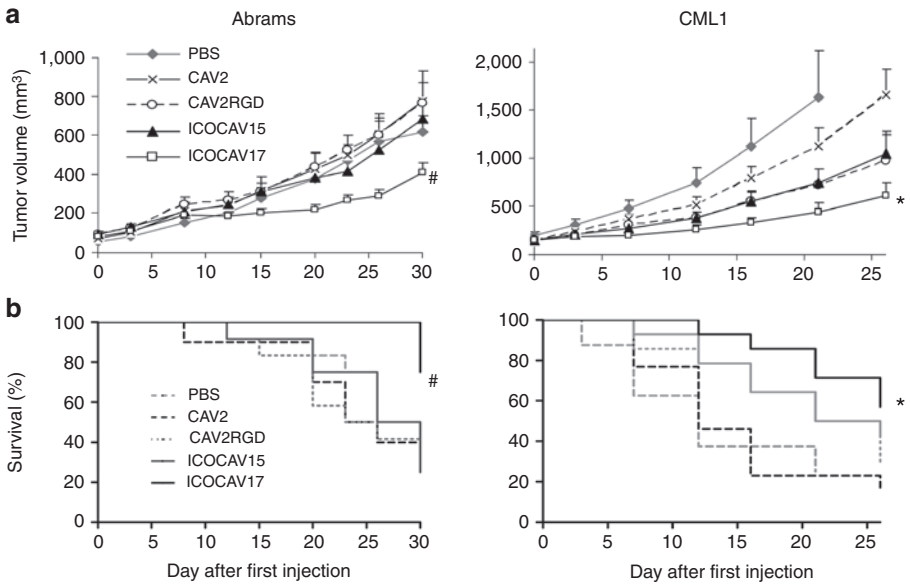

Figure 4 Efficacy and survival after canine adenovirus intratumor injections. Nude mice bearing canine subcutaneous xenografts of osteosarcoma (Abrams) or melanoma (CML1) were treated with three injections (Day 0, 7, and 14) with phosphate-buffered saline (PBS) or 1×10^{10} viral particles per tumor of CAV2, CAV2RGD, ICOCAV15, or ICOCAV17. (**a**) Mean tumor volume values ± SE are plotted ($n = 10$–12). (**b**) Kaplan–Meier survival curves. The end point was established at a volume of ≥500 mm^3. #Statistical significance between ICOCAV17 and PBS, CAV2, CAV2RGD, and ICOCAV15 ($P < 0.05$) by two-tailed unpaired Student's *t*-test. *Statistical significance between ICOCAV17 and PBS and CAV2 ($P < 0.05$) by two-tailed unpaired Student's *t*-test.

Table 1 Summary of patients

Patient ID	Tumor type	Chemotherapy concomitant treatment	Neutralizing antibody titer (days posttreatment)					Virus load in whole blood (vp/ml) (days posttreatment)					Response		
			0	3–5	7–10	11–15	>15	0	1–2	3–4	5–10	>15	RECIST (%)	Other criteria[a] (virus bioactivity)	Survival (days)
Case I	Infiltrative adenoma	No	80	640			32,000	0	1.1×10^5	3.5×10^4		0	PR (−51%)	Improve QoL	>300[c]
Case II	Osteosarcoma	No	2,560	5,120	128,000	256,000		0	1,830	<500	<500		SD	Stable QoL (primary tumor and lung metastasis necrosis)	11
Case III	Mast cell tumor	Toceranib (TKI)[b]	640	1,280	1,280								PR (−70%)	Worse QoL	10
Case IV	Osteosarcoma	Toceranib (TKI)[b]	160		16,000	256,000	512,000	0	1.2×10^5	9.8×10^5		0	PD	Stable QoL (tumor growth stabilization at inoculation site)	70
Case V	Fibrosarcoma	No	80	160	32,000		16,000	0	6.4×10^5	2.6×10^5	1,860	0	SD	Stable QoL (temporally tumor stabilization→ surgical resection)	>200[c]
Case VI	Hepatic endocrine carcinoma	No	ND	20	5,120	21,000	32,000	0	6.3×10^6	2.8×10^6	2.7×10^4	0	SD	Stable QoL (tumor necrosis induction)	22

ND, nondetectable; PR, partial response; PD, progressive disease; SD, stable disease; TKI, tyrosine kinase inhibitor.
A summary of patient tumor type, concomitant chemotherapy treatment, neutralizing antibody titers, viral load in whole blood, treatment responses evaluated by RECIST 1.1 criteria, a health related quality of live questionnaire and virus bioactivity and survival of patients after treatment. [a]Health-related quality of life questionnaire (QoL). [b]2,75 mg/kg/PO/48 hours. [c]Patients still alive at the moment of submission of this manuscript.

virus inoculation (1 month previous to current submission), progressive disease was observed with a tumor volume similar to that at the start of treatment.

Clinical case II. A 7-year-old entire male Ibizan Warren Hound was referred to the Veterinary Hospital with a large humeral mass on the right proximal humerus compatible with OS. Owner reported that lesions started being evident 1 month before, although normal dog activity had not been compromised until 1 week before the visit. Humerus fracture and multiple lung metastases were detected by radiography (**Figure 6a**). Patient presented with normal appetite, alert status, biochemistry, coagulation, and hematologic profiles, except for an increase in alkaline phosphatase. Owner declined euthanasia and conventional treatment protocols. The dog was selected for ICOCAV17 treatment.

Treatment and response: ICOCAV17 was administered using echoguidance within four points aiming at the primary tumor, although swelling hindered accurate echographic differentiation between normal and tumor tissue. Mild temporary swelling with turgor at the injection sites was observed for 48 hours which reverted afterwards. No signs of systemic toxicity were noted throughout the treatment. Appetite and alert status remained unaltered. Tumor size did not show evidence of decrease by echo- or radiographic imaging. On day 10 after administration, patient showed an open and bleeding wound distal to the administration points (**Figure 6a**). Signs of self-trauma on this site were evident. Due to the poor prognosis and the presence of this wound, the dog was euthanized. Histopathology examination showed large necrotic tumor areas (**Figure 6a**) around the points of virus administration, whereas a nontumor area injected accidentally during echoguided administration only showed minimal signs

Figure 5 Treatment response after a single intratumoral administration of ICOCAV17 in an infiltrative adenoma canine patient. Patient I was admitted to the Veterinary Hospital with urinating problems due to a mass in the prepuce skin. Previously excised relapsing adenoma was diagnosed. A dose of 1×10^{12} viral particles of ICOCAV17 was administered intratumorally (Day 0). At that time, the tumor size was $5.6\times5\times3.5$ cm. Six months after treatment, the tumor size had reduced by 51% (RECIST) and was $2.9\times2.8\times2.2$ cm. Tumor size measured by caliper (left) and the depth measured by echographic imaging (right) at days 0 and 180 after treatment, are shown. Right panel: #tumor tissue; *normal tissue. A scale in centimeter is shown in the echographic images.

of bleeding with lack of necrosis. Moreover, necrotic areas in a metastatic nodule of the lung were observed. Virus replication was confirmed by immunohistochemistry for Ad late proteins in both injected tumor and lung metastasis (**Figure 6b**). Healthy adjacent muscular tissue showed no evidence of virus presence (**Figure 6b**).

Clinical case III. A 7-year-old entire male Labrador Retriever was admitted to the Veterinary Hospital with a relapsing cutaneous thoracic mast cell tumor confirmed by fine needle aspiration. Conventional chemotherapy (Vinblastine, Prednisone, and Lomustine) and tyrosine kinase receptor inhibitor (Toceranib) were applied for one and a half month with no response. Tumor started bleeding, ulcerated and progressed, reaching a threefold volume increase since relapse. The dog was selected for investigational therapy with ICOCAV17. As chemotherapy and hyaluronidase synergy has been reported,[32,33] and considering the fast tumor progression and the experience with the two previous cases, Toceranib was used concomitantly to seek chemosensitization with hyaluronidase.

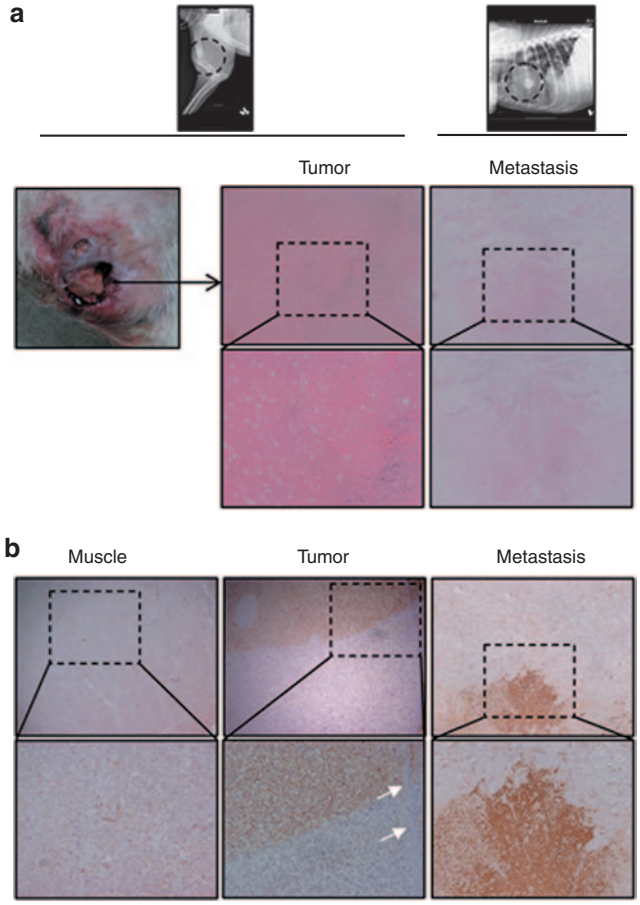

Figure 6 Histopathology and immunohistochemistry staining of healthy tissue, primary tumor, and lung metastasis of an osteosarcoma patient (Case II). Patient II suffered an osteosarcoma in the right front extremity. ICOCAV17 was intratumorally injected in four different sites by echoguidance. (**a**) Euthanasia due to a self-traumatic wound (left panel) was performed 11 days after administration. Broad areas of necrosis were detected in the primary tumor but also in a lung metastatic nodule in the anatomopathological study (central and right panel, respectively). (**b**) Ad detection (brown precipitate) was performed by immune staining using an anti-adenovirus late protein antibody in deparaffinized sections from both, primary and metastatic lesions (central and right panel, respectively). A fibrotic barrier (magnified area; white arrows) is observed in the tumor. Samples from healthy tissue surrounding injected areas were also stained against adenovirus late proteins with no Ad detection (left panel). (**a** and **b**) Upper panel: original magnification ×40. Lower panel: original magnification ×200.

Treatment and response: previrus administration; hematological and biochemical analysis showed mild increase in alanine aminotransferase, alkaline phosphatase, anemia, a hematocrit of 26%, and thrombocytopenia (1.2×10^5 platelets/μl). ICOCAV17 was injected in 10 different points within the thoracic tumor mass. Severe tumor swelling was observed for 48 hours postvirus inoculation. However, tumor necrosis and progressive reduction in tumor volume were evident from day 3 postinoculation until day 10. Hematological and biochemical parameters did not change for the first 7 days after virus inoculation, but later the patient developed progressive renal and hepatic failure. Due to the inflammatory nature of mast cells, the organ failure was attributed to the extensive lysis of mast cell tumor cells and the prolonged unstable general condition (tumor bleeding with low hematocrit and thrombocytopenia). Euthanasia was performed 10 days after virus administration. At that time, tumor size had reduced by 70%. Necropsy showed infarcts in several organs (kidneys, liver, spleen, and heart) with petechiae and general jaundice. Disseminated intravascular coagulation (DIC) was diagnosed. Disseminated intravascular coagulation is a multifactor induced pathology common in dogs. Multiple causes such as viremia, systemic inflammatory response, or direct endothelial damage, lead to coagulation disorders that can evolve in a disseminated intravascular coagulation.

Clinical case IV. A 7-year-old Golden Retriever entire male, was admitted to the Veterinary Hospital with a humeral OS. Limb amputation was declined by the owner. Despite treatment with conventional chemotherapy, nonsteroidal anti-inflammatory drugs, and Toceranib, the disease progressed. Lesions compatible with metastases were observed at the shoulder and spinal bone. The dog was selected for ICOCAV17 investigational treatment. Taking into account the bad prognosis of the patient and the previous results, a combination with Toceranib was considered.

Treatment and response: Before virus administration, the dog presented with hematology and biochemistry profile within normal levels, except for mild elevation of alkaline phosphatase. After intratumoral administration of ICOCAV17 within the primary humeral lesion, swelling of injected areas was observed followed by a control of tumor growth restricted to the injected areas, whereas enlarging of tumor was observed in the surrounding areas. No toxicity-related symptoms were observed through the treatment. No signs of bioactivity or benefit in terms of quality of life were observed and patient was euthanatized 2 months postvirus injection due to progressive disease. Virus replication could not be demonstrated by immunohistochemistry at this time point.

Clinical case V. A 15-year-old Catalan Sheep Dog spayed female was admitted to the Veterinary Hospital with a history of right leg subcutaneous fibrosarcoma at the distal ulna area, previously

treated by surgery and radiotherapy. Limb amputation was declined by the owner. Biochemistry and hematology analysis were within reference limits and physical examination did not show any disorders. Due to the previous case results, in an attempt to avoid tumor relapsing and to study virus replication in a short time period after virus injection, the dog was selected for investigational treatment in a neoadjuvant setting before surgery.

Treatment and response: ICOCAV17 was inoculated at 6 points within the tumor. Initial swelling of the tumor was observed, followed by tumor progression 10 days after virus injection. No adverse events were observed. Fifteen days after administration, tumor was surgically excised. Immunohistochemistry showed areas of virus replication in the subcutaneous tumor tissue (**Figure 7**, left panel), although tumor areas without virus replication were also observed (**Figure 7**, right panel). The dog recovered normally from surgery and after 8 months (last check up, 1 month before current submission) she had no evidence of tumor relapse.

Clinical case VI. A 15-year-old small cross bred entire male was referred to the Veterinary Hospital with a 2-year history of multiple subcutaneous and hepatic nodules. The treatment with steroidal anti-inflammatory drugs had held the disease stable, however tumors were progressing during the last 2 months. Subcutaneous nodules on both flanks, below the jaw, and in the cervical area were observed. Thoracic radiographs and abdominal ultrasound showed nodules on the liver, kidneys, and lungs. A marked alkaline phosphatase increase and normal levels of alanine aminotransferase were observed on biochemistry, and hematology showed a hematocrit of 25.5% and mild nonregenerative anemia.

Treatment and response: Two subcutaneous nodules, one on each flank, were injected with 5×10^{11} vp of ICOCAV17 each. No adverse effects were observed. Neutrophil count increased on day 2, presumably due to mild local reaction. The turgidity of the injected nodules decreased, however, in the last check up, only a 14% reduction in tumor volume was observed in one, with an increase of 7% in the other. The progression of the disease led to death of the patient 22 days after administration due to cardiac arrest. We were not able to detect virus replication in any of the tumors analyzed, however, when the percentage of necrotic area was analyzed, a twofold significant increase within the injected tumors was observed (**Supplementary Figure S2 and Supplementary Materials and Methods**).

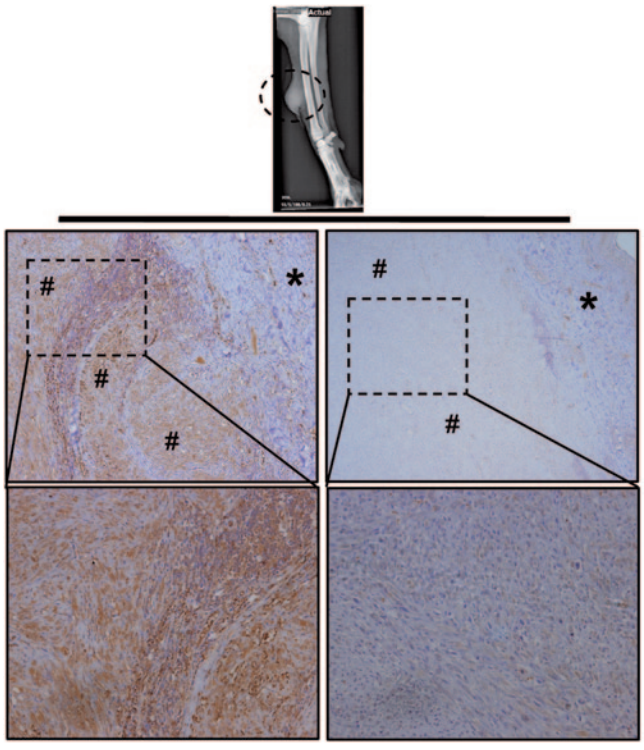

Figure 7 Immunohistochemistry staining of fibrosarcoma tumor from patient V. A Catalan Sheep Dog with a relapsing fibrosarcoma at the distal ulna area of the right leg was admitted to the Hospital. A neoadjuvant setting of virotherapy with ICOCAV17 was performed injecting the virus before surgical resection. Tumor was resected 15 days after injection and embedded in paraffin. Tumor sections were stained with anti-adenovirus late protein antibody. Left panel: virus was detected (brown precipitate) in subcutaneous tumor section. Right panel: tumor section staining did not result in virus detection. (*) skin, (#) tumor tissue. Upper panel: original magnification ×40. Lower panel: original magnification ×200.

Neutralizing antibodies (Nabs) and virus in whole blood and in body secretions

We performed a neutralizing assay using serums from patients and canine Ad vector CAVGFP (wild-type capsid) (**Table 1**). All patients, except patient VI, had detectable Nabs against canine Ad before treatment, which was expected due to vaccination with CAV-2. After treatment, Nabs titer progressively increased until the last follow-up for all patients except Case V. Virus load in whole blood was analyzed by quantitative polymerase chain reaction (PCR) (**Table 1**) (Case III not available). ICOCAV17 was detected early after administration and progressively decreased in time, with the latest positive samples found 7 days after administration (Cases IV and VI). Body secretions (urine, saliva, and feces) were analyzed by anti-hexon staining (daily for the first 4 days postadministration). No canine Ad infectious particles were detected at any time.

DISCUSSION

The increasing incidence of cancer in dogs requires new therapies that overcome resistance against conventional treatments. Herein, we constructed ICOCAV17, a cCRAd based on CAV2 for the treatment of a broad spectrum of canine cancers. ICOCAV17 infected tumor cells more efficiently, showed pRb-mediated selectivity, enhanced cytotoxicity *in vitro* compared with control viruses, and inhibited tumor growth in two canine xenografts *in vivo*. Moreover, six canine patients were treated intratumorally. No adverse side events directly associated to ICOCAV17 administration occurred. Two PR and the observation of virus biological activity in four out of six cases warrant further studies with ICOCAV17. Importantly, the similarities shared by ICOCAV17 with its human counterpart,[19] make it appropriate for extrapolating data from a syngeneic and tumor-spontaneous suffering model to humans.

Preclinical characterization showed that RGD-motif insertion enhanced infectivity and propagation of CAV2 in three out of four cell lines. The effect on infectivity of RGD on CAV2 could not be directly extrapolated from previous data with hAds as CAV2 attaches to and enters cells using a different pathway and lacks

an integrin-interacting motif.[34,35] The CAR and integrins influence CAV2 trafficking, although exact mechanisms are still unknown. We did not find a correlation between CAR-expression levels of the cell lines and CAV2 or CAV2RGD infectivity, suggesting, as mentioned before,[34] the existence of other influencing receptors for CAV2. According to the results obtained, the insertion of the RGD motif does not inhibit CAR interaction as we did not observe a decrease in infectivity in any of the cell lines tested. To achieve pRb-E2F-based selectivity,[21,36,37] four imperfect palindromic E2F-binding sites and one Sp-I-binding site were inserted in the endogenous E1a promoter of CAV2RGD and the pRb-binding site of E1a was deleted. The homology between hAd5 and CAV2 E1 proteins has been previously described.[38] The Δ24 deletion in hAd, homologous to the Δ21 deletion in the canine Ad, hinders the virus to release cellular E2F from pRb-E2F complexes, conferring selectivity for cells with free E2F, which are the majority of tumor cells,[37] while restringing viral replication in nonreplicating cells.[21] In this study, the E1a-modified promoter increased virus burst size and enhanced cytotoxicity in tumor cells, while diminished by more than 80% the total virus production in cell cycle-arrested nontumor cells. The correlation of pRB status and permissiveness to ICOCAV15 supports a pRB-pathway regulation similar to ICOVIR15, although coimmunoprecipitation assays would be required to demonstrate that pRB does not bind to the mutated canine E1a, and that the complex pRB-E2F binds to the inserted E2F boxes.

An extracellular matrix rich in HA limits the efficacy of the CRAds hindering viral intratumor spread.[39] Concentrations of HA are elevated in several human[40] and canine tumors.[41] High levels of HA were detected by immunohistochemistry of sections from CML1 or Abrams xenografts, while 17CM98 tumors showed nondetectable HA levels (**Supplementary Figure S3 and Supplementary Materials and Methods**). Human PH20 hyaluronidase was inserted instead of isogeneic canine hyaluronidase for two reasons: hPH20 is active at a neutral pH whereas canine PH20 exhibits hyaluronidase activity at an acidic pH[42] and CAV2 is already a xenogeneic DNA for the dog. In order to link PH20 expression to CAV replication, we inserted the human PH20 under the control of the canine IIIa protein splicing acceptor which was isolated by sequence alignment with hAd5. Thus, ICOCAV17 represents the first armed canine oncolytic Ad. *In vitro* assays did not show any replication impairment for ICOCAV17 compared with ICOCAV15. A therapeutic advantage for the PH20-armed virus was observed in efficacy studies in two canine xenografts. Detection of virus over paraffin-embedded tumors was performed at the experiment end point, when animals were sacrificed (**Supplementary Figure S1 and Supplementary Materials and Methods**), which may have decreased the possibilities to detect virus. However, a slight increase in the positive area of tumors treated with ICOCAV17 compared to the other viruses was observed, mainly in Abrams tumors, suggesting an enhanced dissemination due to the Hyaluronidase activity.

The toxicity of cCRAds in mice had not been characterized before. Herein, canine viruses induced an important systemic toxicity with marked thrombocytopenia and body weight loss that was aggravated when using RGD-modified viruses. These results suggest that the toxicity could be related to the capsid. The modifications of the E1a promoter were able to reduce by more than 80% the viral production in a cell-cycle arrested cell line, but they were not able to reduce systemic toxicity in Balb/C mice. Thus, reinforcing the hypothesis of a capsid-related toxicity. However, the lack of an antibody against canine E1a hinders the possibility to elucidate the impact of E1a in this toxicity. Further, contrary to the results obtained in dogs by Smith *et al.*,[18] the biodistribution performed in mice showed no specific liver tropism for canine viruses. Moreover, the RGD modified fiber increased the presence of virus in some organs and the persistence in blood, suggesting a change in the virus tropism with a slight liver detargeting. A possible explanation might be that CAV2 remains bound to mouse blood cells without being so efficiently cleared by the liver as are hAds. This could be accentuated for CAV2RGD, thus allowing both viruses to reach multitude of body organs. In whole, these results discouraged us to use the intravenous administration route.

Our main aim was to treat canine patients with a fully-replication competent Ad. Six patients with different tumor types were enrolled in an investigational treatment. The dose of 1×10^{12} vp per animal administered intratumorally was estimated, using a 10 times lower dose than a well-tolerated dose in mice adjusted by weight. We did not reinject canine patients as we had already observed an antitumor response in Case I and III within 3 days postadministration. Moreover, 2×10^{12} vp of OCCAV had been administered intravenously in dogs with no signs of toxicity.[18]

Biochemistry, hematology, and coagulation analysis as well as physical examination were performed daily for at least 4 days after administration. No signs of toxicity associated to ICOCAV17 were observed, even when virus titers reached 10^6 vp per milliliter of blood. The lytic virus activity in tumors caused adverse side events in Case II and III. Case II patient suffered a self-traumatic wound, possibly due to the pain induced by the necrotic tumor tissue. Patient III suffered a disseminated intravascular coagulation as a result of a prolonged bleeding and a massive tumor lysis. To achieve better outcomes, patients with lower tumor loads would be desirable and an accurate selection and control of patients with proinflammatory tumors should be addressed. The immunohistochemistry of nontumor tissue located near injected sites from Case II did not show any evidence of virus replication and no evidence of necrosis in the healthy tissue was detected under macroscopic and microscopic examination. No pathology was found in healthy areas of tissue surrounding the injected sites of any patient. These findings support the E2F/Δ21-conferred selectivity observed *in vitro* and the good tolerance to ICOCAV17 injected intratumorally.

RECIST has been questioned to measure virotherapy efficacy[43] as viruses induce tumor swelling, which can be misinterpreted as progression. Other criteria, based on health-related quality of life,[44] or overall survival have been proposed. Efficacy was seen in Case I and III with a 51% and 70% of reduction in size, respectively. Benefits of the concomitant treatment in Case III should be clarified in future studies. Moreover, a benefit in terms of quality of life was clearly observed in Case I where dysuria disappeared at day 3. The necrosis associated to viral replication suggests virus activity in Case II. While in Case VI, tumor necrosis could not be linked to viral replication. Case IV and V did not show such a marked benefit, although virus replication was found in

the tumor of patient V. Temporary tumor growth stabilization in both patients was observed. The tumor of Patient V was surgically resected 15 days after viral administration. The recovery from the surgical procedure was normal and no tumor relapse was observed at a follow-up 8 months later. This reinforces the safety of the treatment with ICOCAV17 and may suggest a benefit in terms of progression-free survival.

Although tumors use multiple pathways to suppress the immune system, oncolytic viruses could provide intratumoral danger signals that spark an immune response.[45] Our most evident antitumor responses were found in adenoma and mastocitoma patient dogs. Whether the benign characteristics of these tumors are associated with a lower immunosuppression that could facilitate antitumor immunity remains to be studied.

Previous studies suggest that pre-existing immunity against the virus may increase the safety of the treatment, while efficacy by direct administration may not be inhibited.[14,46] Case II had the highest Nabs at the baseline but ICOCAV17 induced necrosis in the primary tumor and in a metastatic lung lesion. This suggests a systemic transport of infective particles even in the presence of Nabs. The higher tumor necrosis and viral systemic dissemination in Case II compared to Case IV, could be associated to higher cell permissiveness to ICOCAV17 replication and the higher accessibility of lung metastasis compared to bone metastases. Recently, Factor X has been described to protect hAd5 from Nabs[47] but, the interaction of CAV2 capsid with canine blood factors remains largely unexplored. Levels of Nabs increased progressively until the last measurement in all patients except for Case V. This exception could be associated to the tumor resection that removed the main virus load. Extended presence of virus in blood has been suggested as a sign of virus replication. Oncolytic effect was evident for at least 6 months (Case I), although we were not able to detect viremia later than 7 days in any case. Virus load in blood decreased progressively in all patients. Therefore, we consider a rapid clearance of circulating cCRAds from blood. We could not find a correlation between virus load in blood, Nabs levels, and antitumor activity or toxicity, pointing at permissiveness to CAV replication as a key factor for efficacy. Accordingly, IC_{50} values (**Figure 2**) suggest a very heterogeneous permissiveness to CAV replication. Even when the tumor cells came from the same tumor type (Abrams and D17 from OS, and CML1 and 17CM98 from melanoma), IC_{50} values were very different. Furthermore, no infectious particles were detected on any of the body fluids analyzed, suggesting a low viral leakage from the tumor and diminishing the shedding risk. However, special care must be undertaken if bleeding or effusions are observed.

In summary, intratumorally treatment of dogs with ICOCAV17 was well tolerated and efficacy was observed in an infiltrative adenoma and a mast cell tumor. ICOCAV17 replicated in tumors and caused tumor necrosis. Enrolling patients with less advanced disease could improve efficacy and reduce adverse events. Finally, dogs with cancer should be considered as a valuable model for human virotherapy.

MATERIALS AND METHODS

Recombinant adenoviruses. **Figure 1a** shows a schematic diagram outlining the structure of the viruses used in this study. pTG5412 containing the wild-type canine adenovirus serotype 2 (CAV2) genome and CAVGFP,[22] a canine vector expressing green fluorescence protein, were a kind gift of Dr Eric Kremer (Institut de Génétique Moléculaire de Montpellier, Montpellier, France). We have generated pCAL-CAV2 using a cut and repair homologous recombination in yeast.[48] pCAL-CAV2 contains the CAV2 genome and the elements needed for selection, amplification, and homologous recombination in yeast (*Saccharomyces cerevisae* YPH857). To this aim, we amplified CAL,[49] a fragment containing the centromere, an autonomously replication sequence "ARS", and a yeast selection gene (Leucine), and we inserted two homologue sequences to pTG5412 in 5′ and 3′. Next, pTG5412 was partially digested with Not I. pCAL-CAV2 was generated by homologous recombination between CAL fragment and the partially digested pTG5412.

CAV2RGD has an RGD motif (CDCRGDCFC) inserted in the Hi-loop (nucleotide position 28110) of the CAV2 fiber. CAV2RGD was generated taking advantage of a unique Sal I site present in pCAL-CAV2. To this aim, two annealing PCRs were performed. First, the RGD motif and a 5′ homologue sequence to pCAL-CAV2 were generated. Then, a second PCR to insert a homologue sequence to pCAL-CAV2 in 3′ was performed using the product from PCR 1 as a template. By homologous recombination, the final product was cloned in Sal I-digested pCAL-CAV2, generating pCAL-CAV2RGD.

To generate ICOCAV15, a fragment of the CAV2-E1a promoter containing four E2F-binding site hairpins (underlined), one Sp-1 binding site (underlined and italics type), and a PmeI restriction site (boldface type) (5′-tcggcggctcgtggctc*tttggc*ggcaaaaagga*tttcgc*gcgtaaaagtggttcgaagtactcg gcggctcgtggctc*tttcgc*ggcaaaaagga*tttggc*gcgtaaaagtggacagtt**gtttaaac**cgacca caaac*cccgccc*agcgtcttgtcattggcgtcga - 3′) following nucleotide 403 of CAV2 genome, and a deletion of 21 base pairs (nucleotide positions 818–838), was designed and cloned in pUC57 flanked by two Xma I restriction sites (GenScript, Piscataway, NJ). A unique Swa I site was used to digest pCAL-CAV2RGD. Homologous recombination was performed between SwaI digested pCAL-CAV2RGD and the fragment obtained from Xma I digestion of pUC57.

To create the PH20 expressing canine adenovirus, a PCR product flanked by two homologue sequences downstream ICOCAV15 fiber protein and containing the CAV2 IIIa protein splicing acceptor (5′-ggccggccctatgaggaagaggagaaccctgatggctccgtctcatttcaacagc - 3′), the human PH20 cDNA, and a polyadenilation signal, was generated by three annealing reactions and inserted by a cut and repair homologue recombination in yeast using the unique Sal I site of pICOCAV15. The viral genomic structures were verified by sequence analysis. All viruses were generated, plaque purified, and amplified in DK28Cre cells. All viruses were purified on CsCl gradients according to standard techniques.

Cell lines. DK28Cre[22] cells were a kind gift of Dr Eric Kremer (Institut de Génétique Moléculaire de Montpellier). Abrams canine OS cell line and 17CM98 and CML1 canine melanoma cells were provided by Dr David Vail (School of Veterinary Medicine, University of Wisconsin-Madison, Wisconsin). D17 canine OS cells were obtained from the American Type Culture Collection (Manassas, VA). DEK are an established primary canine cell line obtained from CELLnTEC (CELLnTEC Advanced Cell Systems AG, Bern, Switzerland). All cells, except DEK, were cultured at 37 °C under 5% CO_2 in Dulbecco's modified Eagle's medium supplemented with antibiotic solution (100 U/ml penicillin G and 100 U/ml streptomycin) and 5% fetal bovine serum. DEKs were cultured at 37 °C under 5% CO_2 in CnT-09 medium from CELLnTEC (CELLnTEC Advanced Cell Systems AG). All cells lines were routinely tested for mycoplasma presence.

Protein expression analysis. Cells were seeded in six-well plates. Whole-cell protein extracts were prepared when tumor-cell cultures reached 80% of confluence or 20 days after confluence for DEKs by incubation in ice-cold radioimmunoprecipitation assay lysis buffer (150 mmol/l NaCl, 1% Nonidet NP-40, 0.5% deoxycholate, 0.1% sodium dodecyl sulfate, 50 mmol/l Tris, pH 8.0), containing phenylmethylsulfonylfluoride (1 mmol/l),

sodium orthovanidate (1 mmol/l), aprotinin (1%), and leupeptin (20 μg/ml) for 1 hour at 4 °C. Clarified samples (25 μg/lane) were separated by a 6.5% sodium dodecyl sulfate–polyacrylamide gel electrophoresis and transferred to a nitrocellulose membrane (GE Healthcare, Arlington Heights, IL). Rb protein detection was performed by immunoblotting membranes using a monoclonal anti-Rb primary antibody (Mouse, Clone G3-245; BD PharMingen, San Jose, CA) and a sheep anti-mouse antibody conjugated with horseradish peroxidase (GE Healthcare, Little Chalfont, UK). A mouse monoclonal anti-α-tubulin antibody (Clone DM1A; Sigma-Aldrich, St Louis, MO) and a sheep peroxidase-conjugated anti-mouse antibody (GE Healthcare) were used for immunoblotting of α-tubulin as a loading control.

Infectivity assay. Abrams or D17 cells (80,000) or 17CM98 or CML1 cells (30,000) were seeded in 96-well plates. After 24 hours, cells were infected in triplicate with serial dilutions of CAV2 or CAV2RGD, starting from 1,000 vp per cell. After 24 hours, medium was removed and immune staining against hexon protein was performed according to an anti-hexon staining-based method.[17] Infected cells expressing hexon protein were counted in the same dilution for both viruses in wells, showing a number of infected cells between 10 and 100, the ratio between CAV2RGD and CAV2 was calculated in triplicate.

Production assays. The selectivity of ICOCAV15 was measured by comparing total production yields in differentiated DEK. DEK become cell-cycle arrested when they are confluent.[28] DEK express cell cycle exit and terminal differentiation markers (p21, p27, Involucrin, Loricrin, and Dsg-1) progressively since they reach confluence.[28] DEK were seeded in 24-well plates and cultured for 20 days at 37 °C and 5%CO_2 with CnT-09. Medium was removed thrice a week and fresh medium was added.

For virus production, differentiated DEK were infected with 8 tu/cell, CML1, D17 cells were infected with 20 tu/cell, and Abrams and 17CM98 with 30 tu/cell of each virus to allow for 80 to 100% infection. After 4 hours, infection medium was removed and cells were washed twice with PBS and incubated with fresh medium. Cells and medium (cell extract) were harvested 48 hours postinfection and subjected to three rounds of freeze-thaw lysis. Viral titers of cell extract were determined in triplicate according to an anti-hexon staining-based method[17] in DK28Cre cells.

Measurement of CAR expression by flow cytometric analysis. Briefly, cell cultures (3×10^5 cells) were incubated with the goat anti-mouse CAR polyclonal antibody CXADR according to the manufacturer's instructions (R&D Systems, Minneapolis, MN) at 4 °C for 1 hour. For the visualization of the anti-CAR antibody, a second incubation with donkey anti-goat Alexa Fluor 488 antibody (diluted 1:300; Invitrogen; Life-technologies, Carlsbad, CA) was conducted at room temperature for 1 hour. Cell samples were analyzed for fluorescence with a Gallios Beckman Coulter flow cytometer (Beckman Coulter, Miami, FL) using a 488-nm laser for excitation. All cytometric data were analyzed with FlowJo software (FlowJo. 7.6.5; Tree Star, Ashland, OR).

Assay for hyaluronidase activity. Hyaluronidase activity assay was performed as described previously.[29] In brief, DK28Cre cells were infected with 20 tu/cell of each virus to allow for 80 to 100% infection. Four hours postinfection, medium was removed and cells incubated with fresh medium. After 48 hours, a volume of hyaluronan solution (3 mg/ml) was added to the cell medium and cells incubated at 37 °C. After this, at 0, 1, 2, 3, and 4 hours, aliquots were removed, boiled for 5 minutes, and centrifuged. Five volumes of sodium acetate buffer (0.1% bovine serum albumin) were added to the supernatant to precipitate hyaluronan. After 10 minutes at room temperature, the turbidity was measured at 600 nm. Samples with a known concentration of purified hyaluronidase (400, 40, 4, and 0.4 UI/ml) were used as hyaluronan degradation standard curve.

In vitro *cytotoxicity assays.* Cytotoxity assays were performed by seeding 20,000 D17 cells, 10,000 Abrams, or 5,000 CML1 or 17CM98 cells per well in 96-well plates in Dulbecco's modified Eagle's medium with 5% fetal bovine serum. Cells were infected with serial dilutions starting with 2,000 tu/cell for Abrams, 17CM98 or CML1 cells, or 500 tu/cell for D17 cells. At days 6–8 postinfection, plates were washed with PBS and stained for total protein content (bicinchoninic acid assay, Pierce Biotechnology, Rockford, IL). Absorbance was quantified and the tu per cell required to produce a 50% of inhibition in cell viability (IC_{50} value) was estimated from dose–response curves by standard nonlinear regression (GraFit; Erithacus Software, Horley, UK), using an adapted Hill equation.

In vivo *toxicity and biodistribution study.* Mice for toxicology and efficacy studies were maintained at the facility of the ICO-IDIBELL (Barcelona, Spain), AAALAC unit 1155. All animal studies have been approved by the Institut d'Investigació Biomèdica de Bellvitge Ethical Committee for Animal Experimentation. A single dose of 1×10^{11} vp was injected intravenously into the tail vein of 8-week-old immunocompetent Balb/C male mice in a volume of 150 μl in PBS ($n = 5$). Daily observations for body weight and morbidity were performed. At day 3 postinjection, mice were sacrificed, exsanguinated, and samples were collected. Blood samples were collected by intracardiac puncture and clinical biochemical and hematological determinations were performed by the Clinical Biochemistry and Hematological Services of the Veterinary Faculty at the Autonomous University of Barcelona. For biodistribution analysis, organs were frozen until processing and DNA was purified following the QIAamp DNA Mini Kit (QIAGEN, Valencia, CA) protocol for DNA Purification from tissues. DNA from blood was extracted from 200 μl of whole blood using the QIAamp DNA Blood Mini Kit (QIAGEN). Purified DNA samples were quantified in triplicate by real-time PCR LightCycler480 Roche, using the primers (forward primer: 5′-TGTGGGCCTGTGTGATTCCT-3′ and reverse primer: 5′-CCAGAATCAGCCTCAGTGCTC-3′), and a Taqman probe (FAM-CTCGAATCAGTGTCAGGCTCCGCA-TAMRA), which identify E1A region. Virus loads were calculated using LightCycler v4.05 software (Roche, Basel, Switzerland) and a regression standard curve based on serial dilutions of pCAL-CAV (1×10^7 to 1 vp/μl).

Evaluation of* in vivo *antitumoral efficacy. Subcutaneous Abrams or CML1 canine tumors were established by injection of 2×10^6 cells into the flanks of 6-week-old female Balb/c *nu/nu* mice. Once tumors reached the desired mean tumor volume (100 mm^3 for Abrams tumors and 150 mm^3 for CML1 tumors), mice were randomly distributed into treatment groups (n = 10–12 tumors per group) and treated (experimental day 0) with an intratumoral injection at days 0, 7, and 14 with 25 μl of PBS or 1×10^{10} vp of CAV2, CAV2RGD, ICOCAV15, or ICOCAV17 in a volume of 25 μl in PBS. Mice status was monitored daily during the 3 days after virus administration. Tumor size and mice status were monitored twice a week. Tumor volume was defined by the equation $V\,(mm^3) = \pi/6 \times W^2 \times L$, where W and L are the width and the length of the tumor, respectively. When animals from each group displayed uncontrolled tumor growth, the mice were euthanized.

For Kaplan–Meier survival curves, end point was established at tumor volume of ≥500 mm^3. The survival curves obtained were compared for the different treatments. Animals whose tumor size never achieved the maximum allowed size were included as right censored information.

Patients. Patients with advanced solid tumors (**Table 1**) refractory to conventional treatments or with a bad prognosis under routinely protocols were eligible for oncolytic virotherapy with ICOCAV17. The inclusion criteria were solid, accessible tumors, refractory or with a bad expected response to conventional therapies and no major organ functions deficiencies. Specific exclusion criteria were immune suppressed animals, with liver disease (hyperbilirubinemia, threefold or higher elevated liver enzymes), thrombocytopenia ($<1 \times 10^5$ Plt/μl), hematocrit < 25%, or cardiorespiratory dysfunctions.

Treatment protocol. ICOCAV17 therapy was approved by the Small Animal Internal Medicine Department of the Veterinary Teaching Hospital (Fundació Hospital Clinic Veterinari) of the Autonomous University of Barcelona. Informed consent was obtained from the dog owners.

Once patients were accepted for treatment with oncolytic virus, on the day of treatment, they were isolated in a facility approved for virus administration in the fundació Hospital Clinic Veterinari of the Autonomous University of Barcelona. Animals were isolated until day 4 after virus administration. Tumors were divided in equal in size quadrants and dose was distributed equally. All patients received a single echoguided intratumoral total dose of 1×10^{12} vp of ICOCAV17 diluted in 1 mililiter of sterile PBS. General anesthesia or sedation with local anesthesia was used according to veterinary recommendation. In Case I, II, and VI, no other agents rather than antibiotics or palliative unrelated agents were given. In Case III and IV, concomitant treatment with the same previously administered chemotherapeutic agents was performed (**Table 1**). Patient V was not concomitantly treated with chemotherapy although surgical resection procedure was included on the protocol before starting the treatment.

Monitoring of patients. Patients were monitored daily for the first 4 days. Attitude, appetite, temperature, cardiac and respiratory frequency, and tumor appearance were checked every 8 hours. Biochemical, hematologic, and coagulation (prothrombin time, partial thromboplastin time, and fibrinogen) analysis were performed once a day, as well as blood, urine, saliva, and fecal sampling. After hospitalization, differences in sampling schedule were adapted to practical issues related to owner time availability. In Case III, the patient was held in observation through the whole process due to its hematologic disorders and evident tumor lysis from day 3. Tumor size was assessed by a caliper and echographic imaging. Maximum tumor diameters were calculated according to RECIST v1.1 (ref. [50]): complete response (CR; undetectable tumor after treatment), PR (≥ 30% reduction in the sum of tumor diameters), stable disease (no reduction or increase), and progressive disease (≥ 20% increase in tumor size).

Analysis of viral infective particles from body secretions. Samples from saliva were obtained using the Salivette system (Sarstedt, Numbrecht, Germany). Samples from urine were obtained using a urinary catheter or intravesical injection. Samples of feces were obtained from the rectum. All samples were frozen until processing. The fecal samples were diluted 1/100 W/V in PBS with penicillin and streptomycin and homogenized. Before titering, samples were centrifuged (10,000*g* for 10'). Once centrifuged, viral titers were determined in triplicate according to an anti-hexon staining-based method[17] in DK28Cre cells. Limits of detection were 100 tu/ml of urine or saliva and 10,000 tu/g of feces.

Histopathology and immunohistochemistry. Samples obtained from tumor or healthy tissues (Case II, IV, V, and VI) were fixed in 10% buffered paraformaldehyde for 24 hours and embedded in paraffin. Routine hematoxylin-eosin staining and immunohistochemistry against adenovirus late proteins were performed. Blocks were cut into 4-µm thick sections and were deparaffinized, endogenous peroxidase activity blocked, and antigen retrieval was performed in citrate buffer. After rehydration, sections were blocked for 30 minutes with 20% normal horse serum diluted in PBS 1% bovine serum albumin. Samples were incubated with rabbit anti-late adenovirus proteins polyclonal IgG (Ab6982 Abcam; cross reactivity against CAV2)[17] overnight at 4 °C. Slides were washed thrice in PBS 0.2% Triton X-100 and incubated with EnVision (Dako, Hamburg, Germany) according to the manufacturer's instructions. After washing, sections were developed with diaminobenzidine (Dako Laboratories, Glostrup, Denmark) and counterstained with hematoxylin. Images of sections were captured on a Nikon Eclipse 80i microscope (Nikon Instruments), using the software NIS-Element Basic Research 3.2 (Nikon, Melville, NY).

Neutralizing antibody titer determination. Samples of serum were heated at 56 °C for 30 minutes in order to inactivate complement. Serial dilutions of inactivated samples were performed in free-serum Dulbecco's modified Eagle's medium in 96-well plates in triplicate, starting from 1/10 (limit of detection) for low titer samples to 1/1,000 for high titer samples. A volume of 100 µl containing 1×10^5 tu of CAVGFP, was added to each well and incubated for 1 hour at room temperature. Afterwards, 5×10^4 DK28Cre cells per well were seeded and cultured overnight at 37 °C and 5% CO_2. The neutralizing antibody titer was determined as the lowest degree of dilution that inhibited the cell transduction by more than 50%.

Quantitative real-time PCR for presence of ICOCAV17 in whole blood samples. DNA was extracted from 200 µl of whole blood using the QIAamp DNA Blood Mini Kit (QIAGEN). Purified DNA samples were quantified in triplicate by real-time PCR LightCycler480 Roche, using the primers (forward primer: 5′-TGTGGGCCTGTGTGATTCCT-3′ and reverse primer: 5′-CCAGAATCAGCCTCAGTGCTC-3′), and a Taqman probe (FAM-CTCGAATCAGTGTCAGGCTCCGCA-TAMRA), which identifies E1A region. Virus loads were calculated using LightCycler v4.05 software and a regression standard curve based on serial dilutions of pICOCAV17 (1×10^7 to 1 vp/µl). The limit of quantification for the assay was 500 vp/ml.

Statistical analysis. Statistics were done with SPSS 13.0 software (IBM, Armonk, NY). Two-tailed Student's unpaired *t*-test was used to compare data, except for survival analysis when data was processed with Kaplan–Meyer analysis.

SUPPLEMENTARY MATERIAL

Figure S1. Immunohistochemistry of tumors from *in vivo* efficacy assays in Abrams and CML1 models.
Figure S2. Hematoxilin & Eosin staining of tumors from patient VI.
Figure S3. Hyaluronic acid detection within three canine xenografts tumors.
Table S1. Systemic biodistribution of CAV2 and CAV2RGD in Balb/C mice.
Materials and Methods.

ACKNOWLEDGMENTS

We thank Sergi Trocoli, Mireia Palau, Francesc Gonzalez, Marta Molla, and Carles Prat for valuable clinical advice and the dog owners who willingly participated in our study as well as the volunteers, nursing staff, and clinicians at the Veterinary Hospital, Mercedes Saez for statistical assistance, and Ruth Riches for linguistic assistance. We thank Erik Kremer and Francesc Viñals for providing some reagents. E.L. was supported by a predoctoral fellowship (FPU) granted by the Spanish Ministry of Education and Science. This work was supported by a grant from the Spanish Ministry of Education and Science, BIO2011-30299-C02-01 and PLE2009-0115 from Spanish Ministry of Economy and Competitivity and received partial support from the Generalitat de Catalunya 2009SGR284. No conflict of interest from any of the authors exists.

REFERENCES

1. Patil, SS, Gentschev, I, Nolte, I, Ogilvie, G and Szalay, AA (2012). Oncolytic virotherapy in veterinary medicine: current status and future prospects for canine patients. *J Transl Med* **10**: 3.
2. Hansen, K and Khanna, C (2004). Spontaneous and genetically engineered animal models; use in preclinical cancer drug development. *Eur J Cancer* **40**: 858–880.
3. Russell, SJ, Peng, KW and Bell, JC (2012). Oncolytic virotherapy. *Nat Biotechnol* **30**: 658–670.
4. Jogler, C, Hoffmann, D, Theegarten, D, Grunwald, T, Uberla, K and Wildner, O (2006). Replication properties of human adenovirus *in vivo* and in cultures of primary cells from different animal species. *J Virol* **80**: 3549–3558.
5. Halldén, G, Hill, R, Wang, Y, Anand, A, Liu, TC, Lemoine, NR *et al.* (2003). Novel immunocompetent murine tumor models for the assessment of replication-competent oncolytic adenovirus efficacy. *Mol Ther* **8**: 412–424.
6. Thomas, MA, Spencer, JF, La Regina, MC, Dhar, D, Tollefson, AE, Toth, K *et al.* (2006). Syrian hamster as a permissive immunocompetent animal model for the study of oncolytic adenovirus vectors. *Cancer Res* **66**: 1270–1276.
7. Raper, SE, Chirmule, N, Lee, FS, Wivel, NA, Bagg, A, Gao, GP *et al.* (2003). Fatal systemic inflammatory response syndrome in a ornithine transcarbamylase deficient patient following adenoviral gene transfer. *Mol Genet Metab* **80**: 148–158.
8. Ternovoi, VV, Le, LP, Belousova, N, Smith, BF, Siegal, GP and Curiel, DT (2005). Productive replication of human adenovirus type 5 in canine cells. *J Virol* **79**: 1308–1311.
9. Westberg, S, Sadeghi, A, Svensson, E, Segall, T, Dimopoulou, M, Korsgren, O *et al.* (2013). Treatment efficacy and immune stimulation by AdCD40L gene therapy of spontaneous canine malignant melanoma. *J Immunother* **36**: 350–358.

10. Paoloni, M and Khanna, C (2008). Translation of new cancer treatments from pet dogs to humans. *Nat Rev Cancer* **8**: 147–156.
11. Kirkness, EF, Bafna, V, Halpern, AL, Levy, S, Remington, K, Rusch, DB *et al.* (2003). The dog genome: survey sequencing and comparative analysis. *Science* **301**: 1898–1903.
12. Buonavoglia, C and Martella, V (2007). Canine respiratory viruses. *Vet Res* **38**: 355–373.
13. Decaro, N, Martella, V and Buonavoglia, C (2008). Canine adenoviruses and herpesvirus. *Vet Clin North Am Small Anim Pract* **38**: 799–814, viii.
14. Dhar, D, Spencer, JF, Toth, K and Wold, WS (2009). Effect of preexisting immunity on oncolytic adenovirus vector INGN 007 antitumor efficacy in immunocompetent and immunosuppressed Syrian hamsters. *J Virol* **83**: 2130–2139.
15. Arendt, M, Nasir, L and Morgan, IM (2009). Oncolytic gene therapy for canine cancers: teaching old dog viruses new tricks. *Vet Comp Oncol* **7**: 153–161.
16. Hemminki, A, Kanerva, A, Kremer, EJ, Bauerschmitz, GJ, Smith, BF, Liu, B *et al.* (2003). A canine conditionally replicating adenovirus for evaluating oncolytic virotherapy in a syngeneic animal model. *Mol Ther* **7**: 163–173.
17. Alcayaga-Miranda, F, Cascallo, M, Rojas, JJ, Pastor, J and Alemany, R (2010). Osteosarcoma cells as carriers to allow antitumor activity of canine oncolytic adenovirus in the presence of neutralizing antibodies. *Cancer Gene Ther* **17**: 792–802.
18. Smith, BF, Curiel, DT, Ternovoi, VV, Borovjagin, AV, Baker, HJ, Cox, N *et al.* (2006). Administration of a conditionally replicative oncolytic canine adenovirus in normal dogs. *Cancer Biother Radiopharm* **21**: 601–606.
19. Guedan, S, Rojas, JJ, Gros, A, Mercade, E, Cascallo, M and Alemany, R (2010). Hyaluronidase expression by an oncolytic adenovirus enhances its intratumoral spread and suppresses tumor growth. *Mol Ther* **18**: 1275–1283.
20. Dmitriev, I, Krasnykh, V, Miller, CR, Wang, M, Kashentseva, E, Mikheeva, G *et al.* (1998). An adenovirus vector with genetically modified fibers demonstrates expanded tropism via utilization of a coxsackievirus and adenovirus receptor-independent cell entry mechanism. *J Virol* **72**: 9706–9713.
21. Rojas, JJ, Guedan, S, Searle, PF, Martinez-Quintanilla, J, Gil-Hoyos, R, Alcayaga-Miranda, F *et al.* (2010). Minimal RB-responsive E1A promoter modification to attain potency, selectivity, and transgene-arming capacity in oncolytic adenoviruses. *Mol Ther* **18**: 1960–1971.
22. Kremer, EJ, Boutin, S, Chillon, M and Danos, O (2000). Canine adenovirus vectors: an alternative for adenovirus-mediated gene transfer. *J Virol* **74**: 505–512.
23. MacEwen, EG, Pastor, J, Kutzke, J, Tsan, R, Kurzman, ID, Thamm, DH *et al.* (2004). IGF-1 receptor contributes to the malignant phenotype in human and canine osteosarcoma. *J Cell Biochem* **92**: 77–91.
24. Thamm, DH, Huelsmeyer, MK, Mitzey, AM, Qurollo, B, Rose, BJ and Kurzman, ID (2010). RT-PCR-based tyrosine kinase display profiling of canine melanoma: IGF-1 receptor as a potential therapeutic target. *Melanoma Res* **20**: 35–42.
25. Koenig, A, Bianco, SR, Fosmire, S, Wojcieszyn, J and Modiano, JF (2002). Expression and significance of p53, rb, p21/waf-1, p16/ink-4a, and PTEN tumor suppressors in canine melanoma. *Vet Pathol* **39**: 458–472.
26. Mendoza, S, Konishi, T, Dernell, WS, Withrow, SJ and Miller, CW (1998). Status of the p53, Rb and MDM2 genes in canine osteosarcoma. *Anticancer Res* **18**(6A): 4449–4453.
27. Suzuki, K, Fueyo, J, Krasnykh, V, Reynolds, PN, Curiel, DT and Alemany, R (2001). A conditionally replicative adenovirus with enhanced infectivity shows improved oncolytic potency. *Clin Cancer Res* **7**: 120–126.
28. Kolly, C, Suter, MM and Müller, EJ (2005). Proliferation, cell cycle exit, and onset of terminal differentiation in cultured keratinocytes: pre-programmed pathways in control of C-Myc and Notch1 prevail over extracellular calcium signals. *J Invest Dermatol* **124**: 1014–1025.
29. Gmachl, M, Sagan, S, Ketter, S and Kreil, G (1993). The human sperm protein PH-20 has hyaluronidase activity. *FEBS Lett* **336**: 545–548.
30. Withrow, SJ, Vail, DM and Page, RL (2012). *Withrow & MacEwen's Small Animal Clinical Oncology*, Elsevier/Saunders: St Louis, MO.
31. Simko, E, Wilcock, BP and Yager, JA (2003). A retrospective study of 44 canine apocrine sweat gland adenocarcinomas. *Can Vet J* **44**: 38–42.
32. Bookbinder, LH, Hofer, A, Haller, MF, Zepeda, ML, Keller, GA, Lim, JE *et al.* (2006). A recombinant human enzyme for enhanced interstitial transport of therapeutics. *J Control Release* **114**: 230–241.
33. Baumgartner, G (1998). The impact of extracellular matrix on chemoresistance of solid tumors–experimental and clinical results of hyaluronidase as additive to cytostatic chemotherapy. *Cancer Lett* **131**: 1–2.
34. Soudais, C, Boutin, S, Hong, SS, Chillon, M, Danos, O, Bergelson, JM *et al.* (2000). Canine adenovirus type 2 attachment and internalization: coxsackievirus-adenovirus receptor, alternative receptors, and an RGD-independent pathway. *J Virol* **74**: 10639–10649.
35. Chillon, M and Kremer, EJ (2001). Trafficking and propagation of canine adenovirus vectors lacking a known integrin-interacting motif. *Hum Gene Ther* **12**: 1815–1823.
36. Johnson, L, Shen, A, Boyle, L, Kunich, J, Pandey, K, Lemmon, M *et al.* (2002). Selectively replicating adenoviruses targeting deregulated E2F activity are potent, systemic antitumor agents. *Cancer Cell* **1**: 325–337.
37. Cascallo, M, Alonso, MM, Rojas, JJ, Perez-Gimenez, A, Fueyo, J and Alemany, R (2007). Systemic toxicity-efficacy profile of ICOVIR-5, a potent and selective oncolytic adenovirus based on the pRB pathway. *Mol Ther* **15**: 1607–1615.
38. Shibata, R, Shinagawa, M, Iida, Y and Tsukiyama, T (1989). Nucleotide sequence of E1 region of canine adenovirus type 2. *Virology* **172**: 460–467.
39. Strauss, R and Lieber, A (2009). Anatomical and physical barriers to tumor targeting with oncolytic adenoviruses in vivo. *Curr Opin Mol Ther* **11**: 513–522.
40. Toole, BP (2004). Hyaluronan: from extracellular glue to pericellular cue. *Nat Rev Cancer* **4**: 528–539.
41. Docampo, MJ, Rabanal, RM, Miquel-Serra, L, Hernández, D, Domenzain, C and Bassols, A (2007). Altered expression of versican and hyaluronan in melanocytic tumors of dogs. *Am J Vet Res* **68**: 1376–1385.
42. Sabeur, K, Foristall, K and Ball, BA (2002). Characterization of PH-20 in canine spermatozoa and testis. *Theriogenology* **57**: 977–987.
43. Koski, A, Kangasniemi, L, Escutenaire, S, Pesonen, S, Cerullo, V, Diaconu, I *et al.* (2010). Treatment of cancer patients with a serotype 5/3 chimeric oncolytic adenovirus expressing GMCSF. *Mol Ther* **18**: 1874–1884.
44. Reid, J, Wiseman-Orr, ML, Scott, EM and Nolan, AM (2013). Development, validation and reliability of a web-based questionnaire to measure health-related quality of life in dogs. *J Small Anim Pract* **54**: 227–233.
45. Elsedawy, NB and Russell, SJ (2013). Oncolytic vaccines. *Expert Rev Vaccines* **12**: 1155–1172.
46. Hu, JC, Coffin, RS, Davis, CJ, Graham, NJ, Groves, N, Guest, PJ *et al.* (2006). A phase I study of OncoVEXGM-CSF, a second-generation oncolytic herpes simplex virus expressing granulocyte macrophage colony-stimulating factor. *Clin Cancer Res* **12**: 6737–6747.
47. Xu, Z, Qiu, Q, Tian, J, Smith, JS, Conenello, GM, Morita, T *et al.* (2013). Coagulation factor X shields adenovirus type 5 from attack by natural antibodies and complement. *Nat Med* **19**: 452–457.
48. Giménez-Alejandre, M, Gros, A and Alemany, R (2012). Construction of capsid-modified adenoviruses by recombination in yeast and purification by iodixanol-gradient. *Methods Mol Biol* **797**: 21–34.
49. Sikorski, RS and Hieter, P (1989). A system of shuttle vectors and yeast host strains designed for efficient manipulation of DNA in Saccharomyces cerevisiae. *Genetics* **122**: 19–27.
50. Eisenhauer, EA, Therasse, P, Bogaerts, J, Schwartz, LH, Sargent, D, Ford, R *et al.* (2009). New response evaluation criteria in solid tumours: revised RECIST guideline (version 1.1). *Eur J Cancer* **45**: 228–247.